Measurement report: Size distributions of urban aerosols down to 1 nm from long-term measurements

Chenjuan Deng[1], Yiran Li[1], Chao Yan[2,3,4], Jin Wu[1], Runlong Cai[2], Dongbin Wang[1], Yongchun Liu[3], Juha Kangasluoma[2,3,5], Veli-Matti Kerminen[2], Markku Kulmala[2,3,4], Jingkun Jiang[1,*]

[1]State Key Joint Laboratory of Environment Simulation and Pollution Control, School of Environment, Tsinghua University, 100084 Beijing
[2]Institute for Atmospheric and Earth System Research/Physics, Faculty of Science, University of Helsinki, 00014 Helsinki, Finland
[3]Aerosol and Haze Laboratory, Beijing Advanced Innovation Center for Soft Matter Science and Engineering, Beijing University of Chemical Technology, 100029 Beijing, China
[4]Joint International Research Laboratory of Atmospheric and Earth System Sciences, School of Atmospheric Sciences, Nanjing University, Nanjing, China
[5]Karsa Ltd., A. I. Virtasen aukio 1, 00560 Helsinki, Finland

*_Correspondence to_: Jingkun Jiang (jiangjk@tsinghua.edu.cn)

Abstract. The size distributions of urban atmospheric aerosols convey important information on their origins and impacts. Their long-term characteristics, especially for sub-3 nm particles, are still limited. In this study, we examined the characteristics of atmospheric aerosol size distributions down to 1 nm based on four-year measurements in urban Beijing. Using cluster analysis, three typical types of number size distributions were identified, i.e., daytime new particle formation (NPF) type, daytime non-NPF type, and nighttime type. Combining a power law distribution and multiple lognormal distributions can well represent the sharp concentration decrease of sub-3 nm particles with increasing size and the modal characteristics for those above 3 nm in the submicron size range. The daytime NPF type exhibits high concentrations of sub-3 nm aerosols together with other three modes. However, both the daytime non-NPF type and the nighttime type have a low abundance of sub-3 nm aerosol particles together with only two distinct modes. In urban Beijing, the concentration of H_2SO_4 monomer during the daytime with NPF is similar to that during the daytime without NPF, while significantly higher than that during the nighttime. The concentration of atmospheric sub-3 nm particles on NPF days has a strong seasonality while their seasonality on non-NPF days is less pronounced. In addition to NPF as the most important source, we show that vehicles can emit sub-3 nm particles as well, although their influence on the measured aerosol population strongly depends on the distance from the road.

1 Introduction

Atmospheric aerosol particles originate from both primary and secondary sources, spreading a wide range of sizes from ~1 nm to hundreds of micrometers. Primary sources directly emit particles over a broad size range, and these sources include natural ones such as windblow dust and sea spray and anthropogenic ones such as coal combustion, traffic emissions, and biomass burning. Secondary sources produce mainly fine and ultrafine particles (Kumar et al., 2014). Atmospheric new particle formation (NPF), for example, generates a significant number of particles down to ~1 nm, which have been shown to be ubiquitous in the atmosphere (Zhang et al., 2012). Traffic emissions can contain sub-3 nm particles and those particles are detected when measurements are made near the sources (Ronkko et al., 2017). In urban atmospheric environment mixed with various emissions, the size distributions of atmospheric aerosol particles are dynamic and complex, reflecting contributions from many primary and secondary sources.

For decades of development, size distributions of atmospheric particles larger than 3 nm have been well understood in contrast to limited information about sub-3 nm particles. Whitby tri-modal representation (Whitby, 1978) has been widely used to describe atmospheric aerosol size distributions, i.e., nuclei mode (~5-100 nm), accumulation mode (~100 nm - 2 μm), and coarse mode (>2 μm). These three modes reflect their origins. For instance, nuclei mode particles are considered to be mainly originated from gas-to-particle conversion. As the understanding of nucleation process extends, a number of studies proposed the presence of nucleation mode in the size range of 3-25 nm which overlaps with Whitby nuclei mode (Covert et al., 1996; Hoppel and Frick, 1990; Mcmurry et al., 2000). For instance, both modeling and experimental results showed that nucleation mode is present when NPF events occur in the atmosphere (Mcmurry et al., 2000; Dal Maso et al., 2005; Hussein et al., 2004).

Advancing measurement techniques enables the development of an improved picture of atmospheric aerosol size distributions. Prior to Whitby tri-modal representation, the prevailed size distribution of atmospheric aerosols was the power function model by Junge (Junge, 1963), which was based on measurements using impactors with a large cut-off size (~0.1 μm) and low size resolution. Developing electrical mobility-based techniques provided data for the tri-modal representation by achieving size distribution measurements down to tens of nanometers with high time resolution and high size resolution (Knutson and Whitby, 1975; Whitby and Clark, 1966). Electrical mobility size spectrometers are now widely used to measure atmospheric aerosol size distributions. During the last decade or so, advanced techniques were developed and improved towards measuring sub-3 nm atmospheric aerosols, such as diethylene glycol based electrical mobility spectrometer (DEG SMPS) (Jiang et al., 2011a), particle size magnifier (PSM) (Vanhanen et al., 2011), neutral cluster and air ion spectrometer (NAIS) (Mirme and Mirme, 2013), half-mini differential mobility particle sizer (Half-mini DMPS) (Kangasluoma et al., 2018) and differential mobility analyzer train (DMA train) (Stolzenburg et al., 2017). Among them, DEG SMPS, PSM, and NAIS have been used in a number of field measurements (Deng et al., 2021; Jiang et al., 2011b; Kontkanen et al., 2016; Kontkanen et al., 2017; Sulo et al., 2021).

These developments and applications improve the understanding about size distributions of atmospheric sub-3 nm particles. Jiang et al. (2011b) first measured atmospheric size distributions down to ~1 nm using DEG SMPS during a short-term campaign in Atlanta and showed the sharp concentration decrease of sub-3 nm particles. The measured aerosol size distribution was further verified by simulation and observation in chamber experiments with sulfuric acid and amine clustering conditions (Chen et al., 2012). Studies measured the concentration of sub-3 nm particles using the PSM at various sites from a boreal forest to polluted megacities (Kontkanen et al., 2017; Kontkanen et al., 2016). Despite these progresses, the characteristics of sub-3 nm particles are still limited. For instance, whether sub-2 nm aerosols always exist with high concentrations in the atmosphere is uncertain, although it is generally agreed that ion clusters in this size range are constantly present. DEG SMPS measurements report high concentrations of sub-2 nm aerosols only during NPF periods (Jiang et al., 2011b) while PSM measurements observe sub-2 nm signals all the time and with elevated concentrations during NPF periods (Kontkanen et al., 2016; Kontkanen et al., 2017). This discrepancy can be partly attributed to different principles of these two instruments (Kangasluoma et al., 2020). Long-term measurements in various atmospheric environments together with improved

understanding of their origins will help to better address this. Additionally, extending Whitby tri-modal representation down to sub-3 nm will provide a full picture of atmospheric aerosol size distributions (Kulmala et al., 2021). More importantly, it can provide information on nucleation processes where 1-3 nm is the critical size range, which can contribute to mechanistic, regional, and global atmospheric models.

To reveal the characteristics of atmospheric aerosol size distributions down to ~1 nm, we started long-term atmospheric measurements in urban Beijing since 2018. Key gaseous precursors for the formation of sub-3 nm particles such as sulfuric acid and its clusters are also measured. This study aims to investigate the characteristics of typical aerosol size distributions together with gaseous precursors from the long-term perspective, the representation of the aerosol size distribution down to ~1 nm, and the possible origins of sub-3 nm aerosols. Particularly, this study focuses on the sub-3 nm size range, including its origin and connection with the rest of the submicron size range, especially the nucleation mode and the nuclei mode.

2 Methods

2.1 Measurements

Atmospheric measurements were conducted at two urban sites in Beijing (Fig. 1). Long-term measurements were carried out on the west campus of Beijing University Chemical Technology (BUCT site) since Jan. 2018. This site is situated ~550 m to the west of the 3rd ring Road and ~130 m to the southwest of a road, which is likely influenced by traffic emissions (Lu et al., 2019; Cai et al., 2021b; Deng et al., 2020). Due to instrument maintenance, the data used in this analysis including those from Jan. 16 – May 17 and Oct. 19 – Dec. 26, 2018, Jan. 1 – Mar. 28, 2019, and Jul. 19, 2019 – Dec. 31, 2021 (a total of 1009 available days). In addition, a short-term campaign was conducted on the campus of Tsinghua University (Tsinghua site) during Mar. 7 – Apr. 6, 2016 (a total of 31 available days). Different from the BUCT site, the Tsinghua site is considered to be less influenced by traffic emissions because the closest major road is ~1 km away from this site (Cai et al., 2017b; Cai and Jiang, 2017). There are no significant stationary emission sources nearby both two sites. Details about these two sites can be found in previous studies (Deng et al., 2020; Cai et al., 2017b).

==========

Place Figure 1 Here

==========

Size distributions of atmospheric aerosols in the range of 1 nm – 10 μm (mobility diameter) were measured using a home-made DEG SMPS (1 – 6.5 nm) (Jiang et al., 2011a; Cai et al., 2017a) and a particle size distribution spectrometer (PSD; 3 nm – 10 μm) (Liu et al., 2016). The schematics and pictures of the DEG SMPS and PSD are shown in Fig. S1 in the Supplementary Information (SI).The DEG SMPS is equipped with a core sampling inlet (Fu et al., 2019) for improving their sampling efficiency, a soft X-ray neutralizer (TSI Inc., model 3088), a specially designed miniature cylindrical differential mobility analyzer (Cai et al., 2017a; Cai et al., 2019) for classifying sub-10 nm particles, and a two-stage condensation particle counter which includes a modified DEG-based ultrafine CPC and a conventional CPC (TSI Inc., 3772). The PSD consists of an aerodynamic particle sizer (APS; TSI Inc., model 3321) and two parallel SMPSs using a nano-DMA (model 3085, TSI Inc.) and a long-DMA (model 3081, TSI Inc.), respectively.

Concentrations of sulfuric acid and its clusters were measured using a nitrate chemical ionization time-of-flight mass spectrometers (Aerodyne Research Inc.) (Zheng et al., 2015; Cai et al., 2017b; Lu et al., 2019). The sampling configurations and calibration procedures were reported previously (Lu et al., 2019; Zheng et al., 2015). The NO concentration was measured by a trace gas analyzer (42i-TL, Thermo Fisher). The meteorological data, including the temperature, relative humidity and ambient pressure were measured using local weather station data acquisition system (Vaisala, AWS310).

2.2 Data analysis

Cluster analysis was used to identify typical atmospheric aerosol number size distributions during the measurement period at both sites. Details about this methodology (Beddows et al., 2009; Wegner et al., 2012) are given in the SI. We identified three typical types of aerosol number size distributions in urban Beijing together with H_2SO_4 and its clusters: C1, C2 and C3 types (Figs. S2 and S3). C1 type has high concentration of sub-3 nm aerosols and is mostly observed during NPF periods (e.g., 9-14) on NPF days. The other two types are mostly observed during non-NPF periods. Thus, they are referred as daytime NPF type, daytime non-NPF type, and nighttime type, respectively. Their characteristics will be further discussed in the following section. The measurement days were classified into NPF days and non-NPF days according to the criteria and examples reported previously (Deng et al., 2020).

A combination of power law and multiple lognormal distribution functions was used to fit the measured H_2SO_4 and its clusters and particle number size distributions. When focusing on number size distributions, we fitted only in the submicron size range, because number concentration of coarse mode particles (>2 μm) is comparatively negligible. Note that to be consistent, we used mass diameter when combining size distributions of H_2SO_4 clusters and particles, otherwise mobility diameter is used for particles. The relation between mobility diameter and mass diameter (Ku and De La Mora, 2009), i.e., mobility diameter is 0.3 nm larger than mass diameter, was used to convert mobility diameter for particles into mass diameter. It should be also noted that, in Figs. 2, 3, S3, S6, S7 and S9, the concentration of H_2SO_4 monomers and dimers was converted into $\mathrm{d}N/\mathrm{dlog}d_\mathrm{p}$ using the method by Jiang et al. (2011b).

For sub-3 nm particles, a power law function is used,

$$\frac{\mathrm{d}N}{\mathrm{dlog}d_p} = a{d_\mathrm{p}}^{-b} \quad (1)$$

where d_p is the particle diameter, nm; $\frac{\mathrm{d}N}{\mathrm{dlog}d_p}$ is the number size distribution function, cm^{-3}; a and b are two fitting parameters for the power law function.

Note that the power law function was chosen to fit in the sub-3 nm because it can well capture the monotonic decrease from H_2SO_4 monomer to dimer and then to the sizes representative of aerosol particles. The log-normal distribution function is not a good fit in the sub-3 nm size range (Fig. S4) and especially a "mode" with a peak diameter of ~0.4 nm resulting from such a fit seems not to be reasonable.

For particles above ~3 nm, multiple lognormal distribution functions (Seinfeld and Pandis, 2008) are used:

$$\frac{\mathrm{d}N}{\mathrm{dlog}d_\mathrm{p}} = \sum_{i=1}^{n} \frac{N_i}{\sqrt{2\pi}\mathrm{log}\sigma_{g,i}} \exp\left[-\frac{(\mathrm{log}d_\mathrm{p} - \mathrm{log}\bar{d}_{pg,i})^2}{2\mathrm{log}^2\sigma_{g,i}}\right] \quad (2)$$

where d_p is the particle diameter, nm; N_i, $\bar{d}_{pg,i}$ and $\sigma_{g,i}$ represent total number concentration (cm^{-3}), geometric mean diameter (nm) and geometric standard deviation (dimensionless) within the mode i.

The intensity of NPF is characterized by the particle formation rate, which measures the growth flux through a certain particle size. A balance formula that enhances the evaluation of coagulation scavenging in the presence of high aerosol loadings was used in this study to evaluate the particle formation rate (Cai and Jiang, 2017),

$$J_k = \frac{\mathrm{d}N_{[d_k,d_u)}}{\mathrm{d}t} + \sum_{d_g=d_k}^{d_{u-1}} \sum_{d_i=d_{\min}}^{+\infty} \beta_{(i,g)} N_{[d_i,d_{i+1})} N_{\left[d_g,d_{g+1}\right)} - \frac{1}{2} \sum_{d_g=d_{\min}}^{d_{u-1}} \sum_{d_i^3=\max\left(d_{\min}^3, d_k^3 - d_{\min}^3\right)}^{d_{i+1}^3 + d_{g+1}^3 \le d_u^3} \beta_{(i,g)} N_{[d_i,d_{i+1})} N_{\left[d_g,d_{g+1}\right)} + \left.\frac{\mathrm{d}N}{\mathrm{d}d_i}\right|_{d_i=d_u} \cdot \mathrm{GR}_u \quad (3)$$

Here J_k is the particle formation rate at size d_k, $cm^3 \cdot s^{-1}$, where d_k was 1.5 nm in this study, nm; d_u is the upper size bound of the chosen aerosol population, nm; d_{min} is the smallest particle size detected by particle size spectrometers, nm; $N_{[d_k,d_u)}$ is the number concentration of particles from size d_k to d_u, cm^{-3}; d_i denotes the lower bound of the i^{th} size bin, nm; $\beta_{(i,g)}$ is the coagulation coefficient for the collision of two particles with size of d_i and d_g, $cm^3 \cdot s^{-1}$; and GR_u represents the particle growth rate at size d_u, $nm \cdot h^{-1}$.

An indicator, *I*, represents the intensity of the NPF in atmospheric environment governed by H_2SO_4-amine nucleation, considering the effects of various parameters such as H_2SO_4 concentration, amine concentration, the stability of H_2SO_4-amine clusters, and background aerosols (Cai et al., 2021a). This indicator has been used to reveal the governing factor for the seasonal variations of NPF in urban Beijing (Deng et al., 2020). It was calculated using the method by Cai et al. (2021a) (details can be found in the SI). Together with other evidence, it is used to explore whether the elevation of sub-3 nm aerosols on non-NPF days is due to nucleation process in Sect. 3.2.

3 Results and discussion

3.1 Typical number size distributions of sub-3 nm aerosols

Figure 2 showed three cases of typical types of aerosol number size distributions. The number size distribution function ($dN/d\log d_p$) was at high levels in the sub-3 nm size range of the daytime NPF type size distribution, and the highest value in this case reached up to ~1.1×10^6 cm^{-3}. The $dN/d\log d_p$ decreased from H_2SO_4 monomer, H_2SO_4 dimer to sub-3 nm aerosols, and reached a trough at ~3 nm (note that H_2SO_4 monomer and dimer are included in the size distribution to provide information about the precursors of nucleation process). This trough can be partly caused by aerosol dynamic processes, which have also been simulated by models (Chen et al., 2012; Li and Cai, 2020). After reaching the trough, the $dN/d\log d_p$ slightly increased but then dropped significantly. The $dN/d\log d_p$ showed no significant increase or decrease from ~12 nm until it started to decrease substantially at ~ 300 nm and reached a low level at 1000 nm. In contrast to the daytime NPF type size distributions, the values of $dN/d\log d_p$ in the sub-3 nm size range of the daytime non-NPF type and nighttime type size distributions were substantially low. The concentrations of sub-2 nm aerosol particles were near zero. In the 2-3 nm size range, the $dN/d\log d_p$ of both daytime non-NPF and nighttime types was low while the $dN/d\log d_p$ was high in the larger size range, and higher than that of the daytime NPF type at sizes larger than about 20 nm. Although the daytime non-NPF type and nighttime type showed similar characteristics in the size range above the H_2SO_4 clusters, the H_2SO_4 monomer concentration was higher during daytime than nighttime.

==========

Place Figure 2 Here

==========

From a long-term perspective, the characteristics of the median aerosol number size distributions for each type were similar in four seasons (Fig. S5). For the daytime NPF type, they showed a similarly sharp particle concentration decrease with increasing size in the sub-3 nm size range and local peaks above ~3 nm in four seasons, although the concentration level showed seasonal variations. The seasonal variations of number concentrations of sub-3 nm aerosols will be discussed in the

following section. For the daytime non-NPF and nighttime type, both the pattern and concentration level were similar in four seasons.

The median atmospheric aerosol size distributions for the whole measurement time period can be generally well fitted using a combination function of the power law and the lognormal distributions (Fig. 3 and Figs. S6-7). Figure 3 showed that such combination function generally fitted the median daytime NPF type aerosol size distribution for the four-year measurements well, both in logarithmic and linear scale of ordinate. In Fig. 3(a), the power function depicted the characteristics that the concentrations decrease from H_2SO_4 monomers to ~3 nm particles. Meanwhile, the lognormal function agreed well with the raw distributions. Figure 3(b) showed the tri-modal lognormal distributions more clearly in the linear scale of ordinate. The daytime NPF type size distribution presented three modes, referred as mode 1, mode 2, and mode 3, respectively. Unlike the daytime NPF type, the daytime non-NPF and nighttime types only showed two modes in the number size distributions (Fig. S6-7).

==========

Place Figure 3 Here

==========

Table 1 summarized the fitted functions and their parameters of those median aerosol number size distributions for the four years of measurements in urban Beijing. The combination function consists of the power function and the lognormal distributions. For the power function, the parameters determining the fitting shape of sub-3 nm size distribution are *a* and *b*. With a larger *b* value, the concentrations decrease going from H_2SO_4 monomer to small clusters and further to particles of a few nanometers is shaper, so *b* values were much larger for the daytime non-NPF and nighttime types than the daytime NPF type. For the daytime non-NPF and nighttime types, although their concentration in sub-3 nm size range were similarly low, the concentration decrease from H_2SO_4 monomer to dimer was sharper for the nighttime type, so the *b* value was larger for the nighttime type than for the daytime non-NPF type. Concerning the lognormal distributions, the number concentration of mode 1 and mode 2 particles were much higher than that of mode 3 for the daytime NPF type. The modal diameters of mode 2 and mode 3 for the daytime non-NPF type and nighttime type were larger than those for the daytime NPF type.

==========

Place Table 1 Here

==========

Compared to the Whitby model, our results showed that in Beijing for the daytime NPF type number size distributions, there existed three modes (mode 1, mode 2, and mode 3) in the ultrafine size range. The first two modes are induced by atmospheric nucleation process and they are in the size range of nucleation mode. There was a trough between mode 1 and mode 2 in the daytime NPF type. This is because the nucleation process produces large numbers of small particles and only a fraction of them grows into larger sizes, together with a strong impact of coagulation in the small size range. Mode 3 in the daytime NPF type is mainly from primary emissions (Morawska et al., 1998; Ristovski et al., 1998), which is often called as Aitken mode.

In contrast to daytime NPF type, for the daytime non-NPF and nighttime type, there were only two modes (mode 2 and mode 3) in the ultrafine size range. The modal diameter in mode 2 for the daytime non-NPF and nighttime types was larger than the daytime NPF type. Also, for daytime non-NPF and nighttime types, the range of mode 2 was much broader and the number concentration in this mode was lower than that for the daytime NPF type. These characteristics indicate no influence of atmospheric nucleation process. Note that these fitting parameters are not presumed to be constant because atmospheric processes and emissions vary spatially and temporally.

The accumulation mode (100 nm – 2 μm) was not shown for all the types of number size distributions in Fig. 3 and Figs. S6-7 because their contribution in number concentrations was low. However, the accumulation mode obviously presented in the volume size distributions of all the types, and the concentration was lower for the daytime NPF type compared to other two types (Fig. S8). The accumulation mode particles showed high concentration in the surface area size distributions as well. This indicates their important role for scavenging smaller particles and condensing species.

Additionally, we showed that this combination model performs well in the measured aerosol size distributions in Atlanta (Fig. S9). The combination model captured the sharp particle concentration decrease with an increasing size in the sub-3 nm size range and the modal characteristics above 3 nm size of the daytime NPF type aerosol size distribution in Atlanta.

3.2 Potential sources of sub-3 nm aerosols in urban Beijing

NPF process is the most important source of atmospheric sub-3 nm particles ($N_{sub\text{-}3}$) in urban Beijing. As shown in Fig. 4(a), $N_{sub\text{-}3}$ showed a clear diurnal variation that reached its daily maximum in the noontime on NPF days. The median daily maximum $N_{sub\text{-}3}$ was ~1.1×10^4 cm^{-3} on NPF days in urban Beijing. The observed daytime maximum of $N_{sub\text{-}3}$ results mainly from the formation of the H_2SO_4 clusters driven by SO_2 oxidation through photochemical process during the daytime on NPF days (Fig. 4(c) and (d), Fig. S10). When the NPF events occurred, $N_{sub\text{-}3}$ was overwhelmingly higher than that when there were no NPF events (non-NPF daytime or nighttime). Similar diurnal cycles of $N_{sub\text{-}3}$ and the dominant contribution of NPF process to the sub-3 nm aerosols were also observed in Shanghai, China (Xiao et al., 2015), Po Valley, Italy (Kontkanen et al., 2016), Kent, US (Yu et al., 2014), which are relatively polluted atmospheric environments.

==========

Place Figure 4 Here

==========

The concentrations of sub-3 nm aerosols showed a strong seasonality on NPF days but had no obvious seasonal variations on non-NPF days (Fig. 5 and Fig. S11), supporting that the elevated $N_{sub\text{-}3}$ was introduced by the NPF process. $N_{sub\text{-}3}$ was significantly higher in winter than those in summer on NPF days. The median daytime $N_{sub\text{-}3}$ on NPF days was ~1.2×10^4 cm^{-3} in winter in contrast to ~200 cm^{-3} in summer. However, the more important reason is the much lower NPF intensity in summer because the seasonal variation of $N_{sub\text{-}3}$ on NPF days was consistent with those of H_2SO_4 dimer concentration and the formation rates of ~1.5 nm aerosols (Fig. S12). This indicates that the seasonal variation of the formation process drives the seasonal variation of $N_{sub\text{-}3}$. This seasonal variation is different from that observed in Hyytiälä, a boreal forest site in Finland, in which $N_{sub\text{-}3}$ was the highest in summer or spring and the lowest in winter (Sulo et al., 2021). The highest concentration of small particles in the size range of 1.1 – 1.7 nm in Hyytiälä was observed during summertime, coinciding with the high photochemical and biogenic activity in summer (Sulo et al., 2021).

==========

Place Figure 5 Here

==========

In addition to atmospheric NPF, sub-3 nm aerosols can also be emitted by primary sources, such as traffic emissions. This is relatively easier to explore during non-NPF days. As shown in Fig. 4(a), $N_{sub\text{-}3}$ showed small morning (~6:00-9:00) and evening (~16:00-19:00) peaks on non-NPF days, roughly corresponding to the traffic rush hours in the morning and evening in urban Beijing. Although number concentrations of sub-2 nm aerosols were very low, those of 2-3 nm aerosols ($N_{2\text{-}3}$) showed diurnal patterns on non-NPF days (Fig. 4(b)), indicating that the morning and evening peaks are more likely due to primary emissions.

The obvious difference of the $N_{2\text{-}3}$ on non-NPF days between the Tsinghua site and the BUCT site, and between the COVID-19 lockdown period and normal period, further supports that vehicles emit 2-3 nm particles (Fig. 6). The morning and evening peaks of $N_{2\text{-}3}$ on non-NPF days were more prominent at the BUCT site (closer to traffic roads) than at the Tsinghua site that is considered to be less influenced by traffic emissions. In addition, we found that $N_{2\text{-}3}$ was much lower during the strict COVID-19 lockdown period at the BUCT site than normal time period. Traffic flows were extremely low during this strict lockdown period, such that traffic emissions were significantly reduced.

A non-NPF case (Mar. 13, 2018) was examined to further confirm that vehicles can emit 2-3 nm aerosols (Fig. 6(b) and (c)). On this non-NPF day, $N_{2\text{-}3}$ started to increase at around 6:00 and reached the maximum at around 8:00 when the concentration of the gas tracer for the traffic emissions, NO, also showed a peak. Furthermore, the NPF indicator, *I*, had low values during this morning time, indicating that the increase of 2-3 nm aerosols was unlikely due to nucleation process (Fig. 6(c)). Previous studies reported that traffic can directly emit sub-3 nm aerosols and thus can be an important source for sub-3 nm aerosols (Ronkko et al., 2017). Our results in urban Beijing support that traffic can emit 2-3 nm particles, but their relative contribution to the total aerosol number is negligible on NPF days.

==========

Place Figure 6 Here

==========

Figure 6 also showed that, unlike secondary formation process, traffic emissions in terms of sub-3 nm aerosols is of local characteristic and its impact on the measured aerosol population strongly depends on the distance between the traffic road and the measurement site. Nucleation and subsequent growth processes exist not only in the atmosphere but also in the exit of pipelines of vehicles (Giechaskiel et al., 2014). In the large-scale atmosphere, the relative homogeneity of sufficient gaseous precursors for nucleation and growth processes enables the burst of sub-3 nm aerosols. The lifetime of sub-3 nm aerosols is extremely short due to strong coagulation effects in urban Beijing (Deng et al., 2021). Thus, sub-3 nm particles directly emitted from traffic are abundant only if one directly measures near the exhaust (Ronkko et al., 2017). This is supported by the fact that significantly less sub-2 aerosols were observed than 2-3 nm aerosols during the traffic rush hour both at the BUCT site and the Tsinghua site, i.e., due to the higher loss rate of sub-2 nm aerosols than 2-3 nm aerosols.

4 Implications

This study describes and interprets aerosol size distributions down to ~1 nm in urban atmospheric environments. Based on the modified Whitby model, we introduce the simplification of aerosol size distributions in sub-3 nm sizes, i.e., the power function. This fitting function captures well the sharp concentration decrease of sub-3 nm particles with an increasing particle size. Although different nucleation mechanisms exist in different atmospheric environments (Sipila, 2010; Jokinen et al., 2018; Lehtipalo et al., 2018; Yao et al., 2018; Yan et al., 2021; Beck et al., 2022), this simplified representation can be applied because concentrations often decrease with an increasing size when going from precursor molecules to small clusters and further to aerosol particle of a few nanometers (Jiang et al., 2011b; Chen et al., 2012; Kulmala et al., 2021).

The aerosol size distributions down to ~1 nm and their representations are important parameters which can contribute to mechanistic, regional and global atmospheric models. For instance, for large-scale or regional models, the aerosol size distributions are initial input parameters to estimate aerosol population or CCN budgets (Von Salzen et al., 2000; Adams, 2002). In some models, the aerosol module often takes the modal representation of aerosol size distributions as input to simulate the aerosol dynamics for better computational speed (Binkowski and Roselle, 2003; Vignati et al., 2004). In urban environments with great complexity of precursors and emission sources, the representation of aerosol size distributions could

be adjusted according to our findings instead of using the traditional three lognormal modal aerosol size distributions. Another benefit is that size distributions ranging from molecular levels to the submicron size range can help to better simulate the NPF and growth mechanisms. For instance, Zhao and coworkers (Zhao et al., 2020) used a comprehensive model to investigate the NPF mechanisms in the Amazon free troposphere. They used measured aerosol size distributions with a lower size limit of ~10 nm to compare to simulated ones. Since sub-3 nm is the critical size range where nucleation occurs, it is needed to cover this size range when comparing simulations with atmospheric measurements. This is more important for urban environment mixed with various processes and more complex than pristine environment. Additionally, the power law function can be readily incorporated in models. For instance, in the global climate models, the observed aerosol size distributions are used to compare with simulated ones (Bergman et al., 2012) and the sub-3 nm size range is the key to simulate nucleation process accurately. However, due to relative scarcity of measured particle size distributions in sub-3 nm around the world, the comparison between observed and simulated results is usually lacking this key size range. Our power law function, as the simplified representation of sub-3 nm size distributions, can extend the observed particle size distributions above 3 nm to sub-3 nm, thus helps to constrain the aerosol module in the global models.

Based on long-term observational results, we addressed whether high concentrations of sub-2 nm aerosols are always present in the atmosphere. We show that concentrations of atmospheric sub-2 nm aerosols are high when NPF events occur. However, they are significantly lower during non-NPF periods (often not detected by DEG SMPS) compared to NPF periods even though the H_2SO_4 monomer concentration is often similar. Different from results measured by DEG SMPS, previous studies reported that high concentrations of atmospheric sub-2 nm aerosols measured by PSM are constantly present in the daytime (Kangasluoma et al., 2020; Kulmala et al., 2021). Although the higher noise-to-signal ratio and higher detection sensitivity of PSM may partly contribute (Kangasluoma and Kontkanen, 2017), considering that there is always high concentration of ion clusters in the atmosphere, the high signal of PSM all the time may be because that it measures both aerosol particles and ion clusters (Kangasluoma et al., 2020; Kulmala et al., 2021).

Additionally, our study implies that although vehicles can be massive in megacities, their direct emissions of sub-3 nm aerosols only influence within the vicinities of traffic roads rather than the large-scale atmosphere. There are studies indicating that vehicles can emit high concentrations of sub-3 nm aerosols as detected by PSM (Ronkko et al., 2017; Okuljar et al., 2021). Similar to previous studies showing that concentrations of ultrafine particles emitted by vehicles decrease significantly as the distance from the roads increases, due to the rapid dilution and strong aerosol dynamic processes such as coagulation and condensation in the atmosphere (Zhu et al., 2002). Our study indicates that the decreasing phenomenon is more significant with respect to sub-3 nm aerosols. Thus, though 2-3 nm aerosols emitted from vehicles were detected by DEG SMPS at both sites in urban Beijing, emissions of sub-2 nm aerosols were barely observed. Future studies measuring the size distributions of sub-3 nm aerosols simultaneously at sites with different distances from traffic roads can be performed to further investigate the impacts of vehicle emissions on atmospheric sub-3 nm aerosols without measurement interferences from ion clusters.

5 Conclusions

In this study, we identify three typical types of number size distributions based on four-year measurements using cluster analysis, i.e., daytime NPF type, daytime non-NPF type, and nighttime type, and investigate their characteristics. The daytime NPF type exhibits high concentrations of sub-3 nm aerosols together with other three modes. The first two modes are induced by atmospheric nucleation process and the third mode in the daytime NPF type is mainly from primary emissions. However, both the daytime non-NPF type and the nighttime type have a low abundance of sub-3 nm aerosol particles together with only two distinct modes because they have no influence of nucleation process. In urban Beijing, the concentration of H_2SO_4 monomer during the daytime with NPF is similar to that during the daytime without NPF, while significantly higher than that during the nighttime. We use a power law distribution and multiple lognormal distributions to represent the sharp concentration

decrease of sub-3 nm particles with increasing size and the modal characteristics for those above 3 nm in the submicron size range. This fitting function also performs well in Atlanta. We show that NPF is the major source of sub-3 nm particles in urban Beijing. In addition to NPF, we find that vehicles can also emit sub-3 nm particles, although their influence on the measured aerosol population strongly depends on the distance from the road.

Data availability

The datasets for this study can be accessible via https://doi.org/10.5281/zenodo.6654175. The details are available upon request from the corresponding author.

Supplement link: the link to the supplement is available at…

Author Contribution

C.D. and J.J. designed the research; C.D., Y.L., J.W., C.Y., Y.L., M.K. and J.J. collected the data; C.D. and J.J. analyzed data with the help from R.C., D.W., Y.C., V.K. and M.K.; C.D. and J.J. wrote the paper with inputs from all co-authors.

Competing interests

The author declares no competing interests.

Acknowledgement

Financial support from the National Science Foundation of China (22188102 and 92044301) and Samsung $PM_{2.5}$ SRP are acknowledged. We also acknowledge the following projects: ACCC Flagship by the Academy of Finland (337549), Academy professorship by the Academy of Finland (302958), Academy of Finland projects (1325656, 311932, 316114, 332547, and 325647), "Quantifying carbon sink, CarbonSink+ and their interaction with air quality" INAR project by Jane and Aatos Erkko Foundation, European Research Council (ERC) project ATM-GTP (742206).

References

Adams, P. J.: Predicting global aerosol size distributions in general circulation models, Journal of Geophysical Research, 107, 10.1029/2001jd001010, 2002.

Beck, L. J., Schobesberger, S., Sipilä, M., Kerminen, V.-M., and Kulmala, M.: Estimation of sulfuric acid concentration using ambient ion composition and concentration data obtained with atmospheric pressure interface time-of-flight ion mass spectrometer, Atmospheric Measurement Techniques, 15, 1957-1965, 10.5194/amt-15-1957-2022, 2022.

Beddows, D. C. S., Dall'Osto, M., and Harrison, R. M.: Cluster Analysis of Rural, Urban, and Curbside Atmospheric Particle Size Data, Environmental Science & Technology, 43, 4694-4700, 10.1021/es803121t, 2009.

Bergman, T., Kerminen, V. M., Korhonen, H., Lehtinen, K. J., Makkonen, R., Arola, A., Mielonen, T., Romakkaniemi, S., Kulmala, M., and Kokkola, H.: Evaluation of the sectional aerosol microphysics module SALSA implementation in ECHAM5-HAM aerosol-climate model, Geoscientific Model Development, 5, 845-868, 10.5194/gmd-5-845-2012, 2012.

Binkowski, F. S. and Roselle, S. J.: Models-3 Community Multiscale Air Quality (CMAQ) model aerosol component 1. Model description, Journal of Geophysical Research: Atmospheres, 108, 10.1029/2001jd001409, 2003.

Cai, R. and Jiang, J.: A new balance formula to estimate new particle formation rate: reevaluating the effect of coagulation scavenging, Atmospheric Chemistry and Physics, 17, 12659-12675, 10.5194/acp-17-12659-2017, 2017.

Cai, R., Zhou, Y., and Jiang, J.: Transmission of charged nanoparticles through the DMA adverse axial electric field and its improvement, Aerosol Science and Technology, 54, 21-32, 10.1080/02786826.2019.1673306, 2019.

Cai, R., Chen, D.-R., Hao, J., and Jiang, J.: A miniature cylindrical differential mobility analyzer for sub-3 nm particle sizing, Journal of Aerosol Science, 106, 111-119, 10.1016/j.jaerosci.2017.01.004, 2017a.

Cai, R., Yang, D., Fu, Y., Wang, X., Li, X., Ma, Y., Hao, J., Zheng, J., and Jiang, J.: Aerosol surface area concentration: a governing factor in new particle formation in Beijing, Atmospheric Chemistry and Physics, 17, 12327-12340, 10.5194/acp-17-12327-2017, 2017b.

Cai, R., Yan, C., Worsnop, D. R., Bianchi, F., Kerminen, V.-M., Liu, Y., Wang, L., Zheng, J., Kulmala, M., and Jiang, J.: An indicator for sulfuric acid–amine nucleation in atmospheric environments, Aerosol Science and Technology, 1-11, 10.1080/02786826.2021.1922598, 2021a.

Cai, R., Yan, C., Yang, D., Yin, R., Lu, Y., Deng, C., Fu, Y., Ruan, J., Li, X., Kontkanen, J., Zhang, Q., Kangasluoma, J., Ma, Y., Hao, J., Worsnop, D. R., Bianchi, F., Paasonen, P., Kerminen, V.-M., Liu, Y., Wang, L., Zheng, J., Kulmala, M., and Jiang, J.: Sulfuric acid–amine nucleation in urban Beijing, Atmospheric Chemistry and Physics, 21, 2457-2468, 10.5194/acp-21-2457-2021, 2021b.

Chen, M., Titcombe, M., Jiang, J., Jen, C., Kuang, C., Fischer, M. L., Eisele, F. L., Siepmann, J. I., Hanson, D. R., Zhao, J., and McMurry, P. H.: Acid-base chemical reaction model for nucleation rates in the polluted atmospheric boundary layer, Proc Natl Acad Sci U S A, 109, 18713-18718, 10.1073/pnas.1210285109, 2012.

Covert, D. S., Wiedensohler, A., Aalto, P., Heintzenberg, J., Mcmurry, P. H., and Leck, C.: Aerosol number size distributions from 3 to 500 nm diameter in the arctic marine boundary layer during summer and autumn, Tellus B: Chemical and Physical Meteorology, 48, 197-212, 1996.

Dal Maso, M., Kulmala, M., Riipinen, I., Wagner, R., Hussein, T., Aalto, P. P., and Lehtinen, K. E.: Formation and growth of fresh atmospheric aerosols: eight years of aerosol size distribution data from SMEAR II, Hyytiala, Finland, Boreal Environment Research, 10, 323, 2005.

Deng, C., Cai, R., Yan, C., Zheng, J., and Jiang, J.: Formation and growth of sub-3 nm particles in megacities: impact of background aerosols, Faraday Discuss, 226, 348-363, 10.1039/d0fd00083c, 2021.

Deng, C., Fu, Y., Dada, L., Yan, C., Cai, R., Yang, D., Zhou, Y., Yin, R., Lu, Y., Li, X., Qiao, X., Fan, X., Nie, W., Kontkanen, J., Kangasluoma, J., Chu, B., Ding, A., Kerminen, V. M., Paasonen, P., Worsnop, D. R., Bianchi, F., Liu, Y., Zheng, J., Wang, L., Kulmala, M., and Jiang, J.: Seasonal Characteristics of New Particle Formation and Growth in Urban Beijing, Environ Sci Technol, 54, 8547-8557, 10.1021/acs.est.0c00808, 2020.

Fu, Y., Xue, M., Cai, R., Kangasluoma, J., and Jiang, J.: Theoretical and experimental analysis of the core sampling method: Reducing diffusional losses in aerosol sampling line, Aerosol Science and Technology, 53, 793-801, 10.1080/02786826.2019.1608354, 2019.

Giechaskiel, B., Manfredi, U., and Martini, G.: Engine Exhaust Solid Sub-23 nm Particles: I. Literature Survey, SAE International Journal of Fuels and Lubricants, 7, 950-964, 10.4271/2014-01-2834, 2014.

Hoppel, W. and Frick, G.: Submicron aerosol size distributions measured over the tropical and south Pacific, Atmospheric Environment. Part A. General Topics, 24, 645-659, 1990.

Hussein, T., Puustinen, A., Aalto, P. P., Mäkelä, J. M., Hämeri, K., and Kulmala, M.: Urban aerosol number size distributions, Atmospheric Chemistry and Physics, 4, 391-411, 2004.

Jiang, J., Chen, M., Kuang, C., Attoui, M., and McMurry, P. H.: Electrical Mobility Spectrometer Using a Diethylene Glycol Condensation Particle Counter for Measurement of Aerosol Size Distributions Down to 1 nm, Aerosol Science and Technology, 45, 510-521, 10.1080/02786826.2010.547538, 2011a.

Jiang, J., Zhao, J., Chen, M., Eisele, F. L., Scheckman, J., Williams, B. J., Kuang, C., and McMurry, P. H.: First Measurements of Neutral Atmospheric Cluster and 1–2 nm Particle Number Size Distributions During Nucleation Events, Aerosol Science and Technology, 45, ii-v, 10.1080/02786826.2010.546817, 2011b.

Jokinen, T., Sipilä, M., Kontkanen, J., Vakkari, V., Tisler, P., Duplissy, E.-M., Junninen, H., Kangasluoma, J., Manninen, H., Petäjä, T., Kulmala, M., Worsnop, D., Kirkby, J., Virkkula, A., and Kerminen, V. M.: Ion-induced sulfuric acid–ammonia nucleation drives particle formation in coastal Antarctica, Science Advances, 4, eaat9744, 10.1126/sciadv.aat9744, 2018.

Junge, C. E.: Air chemistry and radioactivity, 1963, 382-382, 1963.

Kangasluoma, J. and Kontkanen, J.: On the sources of uncertainty in the sub-3 nm particle concentration measurement, Journal of Aerosol Science, 112, 34-51, 10.1016/j.jaerosci.2017.07.002, 2017.

Kangasluoma, J., Ahonen, L. R., Laurila, T. M., Cai, R., Enroth, J., Mazon, S. B., Korhonen, F., Aalto, P. P., Kulmala, M., Attoui, M., and Petäjä, T.: Laboratory verification of a new high flow differential mobility particle sizer, and field measurements in Hyytiälä, Journal of Aerosol Science, 124, 1-9, 10.1016/j.jaerosci.2018.06.009, 2018.

Kangasluoma, J., Cai, R., Jiang, J., Deng, C., Stolzenburg, D., Ahonen, L. R., Chan, T., Fu, Y., Kim, C., Laurila, T. M., Zhou, Y., Dada, L., Sulo, J., Flagan, R. C., Kulmala, M., Petäjä, T., and Lehtipalo, K.: Overview of measurements and current instrumentation for 1–10 nm aerosol particle number size distributions, Journal of Aerosol Science, 148, 10.1016/j.jaerosci.2020.105584, 2020.

Knutson, E. and Whitby, K.: Aerosol classification by electric mobility: apparatus, theory, and applications, Journal of Aerosol Science, 6, 443-451, 1975.

Kontkanen, J., Järvinen, E., Manninen, H. E., Lehtipalo, K., Kangasluoma, J., Decesari, S., Gobbi, G. P., Laaksonen, A., Petäjä, T., and Kulmala, M.: High concentrations of sub-3nm clusters and frequent new particle formation observed in the Po Valley, Italy, during the PEGASOS 2012 campaign, Atmospheric Chemistry and Physics, 16, 1919-1935, 10.5194/acp-16-1919-2016, 2016.

Kontkanen, J., Lehtipalo, K., Ahonen, L., Kangasluoma, J., Manninen, H. E., Hakala, J., Rose, C., Sellegri, K., Xiao, S., Wang, L., Qi, X., Nie, W., Ding, A., Yu, H., Lee, S., Kerminen, V.-M., Petäjä, T., and Kulmala, M.: Measurements of sub-3 nm particles using a particle size magnifier in different environments: from clean mountain top to polluted megacities, Atmospheric Chemistry and Physics, 17, 2163-2187, 10.5194/acp-17-2163-2017, 2017.

Ku, B. K. and de la Mora, J. F.: Relation between Electrical Mobility, Mass, and Size for Nanodrops 1–6.5 nm in Diameter in Air, Aerosol Science and Technology, 43, 241-249, 10.1080/02786820802590510, 2009.
Kulmala, M., Stolzenburg, D., Dada, L., Cai, R., Kontkanen, J., Yan, C., Kangasluoma, J., Ahonen, L. R., Gonzalez-Carracedo, L., Sulo, J., Tuovinen, S., Deng, C., Li, Y., Lehtipalo, K., Lehtinen, K. E. J., Petäjä, T., Winkler, P. M., Jiang, J., and Kerminen, V.-M.: Towards a concentration closure of sub-6 nm aerosol particles and sub-3 nm atmospheric clusters, Journal of Aerosol Science, 159, 10.1016/j.jaerosci.2021.105878, 2021.
Kumar, P., Morawska, L., Birmili, W., Paasonen, P., Hu, M., Kulmala, M., Harrison, R. M., Norford, L., and Britter, R.: Ultrafine particles in cities, Environ Int, 66, 1-10, 10.1016/j.envint.2014.01.013, 2014.
Lehtipalo, K., Yan, C., Dada, L., Bianchi, F., Xiao, M., Wagner, R., Stolzenburg, D., Ahonen, L. R., Amorim, A., and Baccarini, A. J. S. a.: Multicomponent new particle formation from sulfuric acid, ammonia, and biogenic vapors, 4, eaau5363, 2018.
Li, C. and Cai, R.: Tutorial: The discrete-sectional method to simulate an evolving aerosol, Journal of Aerosol Science, 150, 10.1016/j.jaerosci.2020.105615, 2020.
Liu, J., Jiang, J., Zhang, Q., Deng, J., and Hao, J.: A spectrometer for measuring particle size distributions in the range of 3 nm to 10 μm, Frontiers of Environmental Science & Engineering, 10, 63-72, 10.1007/s11783-014-0754-x, 2016.
Lu, Y., Yan, C., Fu, Y., Chen, Y., Liu, Y., Yang, G., Wang, Y., Bianchi, F., Chu, B., Zhou, Y., Yin, R., Baalbaki, R., Garmash, O., Deng, C., Wang, W., Liu, Y., Petäjä, T., Kerminen, V.-M., Jiang, J., Kulmala, M., and Wang, L.: A proxy for atmospheric daytime gaseous sulfuric acid concentration in urban Beijing, Atmospheric Chemistry and Physics, 19, 1971-1983, 10.5194/acp-19-1971-2019, 2019.
McMurry, P. H., Shan Woo, K., Weber, R., Chen, D.-R., and Pui, D. Y.: Size distributions of 3–10 nm atmospheric particles: Implications for nucleation mechanisms, Philosophical Transactions of the Royal Society of London. Series A: Mathematical, Physical and Engineering Sciences, 358, 2625-2642, 2000.
Mirme, S. and Mirme, A.: The mathematical principles and design of the NAIS – a spectrometer for the measurement of cluster ion and nanometer aerosol size distributions, Atmospheric Measurement Techniques, 6, 1061-1071, 10.5194/amt-6-1061-2013, 2013.
Morawska, L., Bofinger, N. D., Kocis, L., and Nwankwoala, A.: Submicrometer and supermicrometer particles from diesel vehicle emissions, Environmental science & technology, 32, 2033-2042, 1998.
Okuljar, M., Kuuluvainen, H., Kontkanen, J., Garmash, O., Olin, M., Niemi, J. V., Timonen, H., Kangasluoma, J., Tham, Y. J., Baalbaki, R., Sipilä, M., Salo, L., Lintusaari, H., Portin, H., Teinilä, K., Aurela, M., Dal Maso, M., Rönkkö, T., Petäjä, T., and Paasonen, P.: Measurement report: The influence of traffic and new particle formation on the size distribution of 1–800 nm particles in Helsinki – a street canyon and an urban background station comparison, Atmospheric Chemistry and Physics, 21, 9931-9953, 10.5194/acp-21-9931-2021, 2021.
Ristovski, Z. D., Morawska, L., Bofinger, N. D., and Hitchins, J.: Submicrometer and Supermicrometer Particulate Emission from Spark Ignition Vehicles, Environmental Science & Technology, 32, 3845-3852, 10.1021/es980102d, 1998.
Ronkko, T., Kuuluvainen, H., Karjalainen, P., Keskinen, J., Hillamo, R., Niemi, J. V., Pirjola, L., Timonen, H. J., Saarikoski, S., Saukko, E., Jarvinen, A., Silvennoinen, H., Rostedt, A., Olin, M., Yli-Ojanpera, J., Nousiainen, P., Kousa, A., and Dal Maso, M.: Traffic is a major source of atmospheric nanocluster aerosol, Proc Natl Acad Sci U S A, 114, 7549-7554, 10.1073/pnas.1700830114, 2017.
Seinfeld, J. and Pandis, S.: Atmospheric Chemistry and Physics. 1997, New York, 2008.
Sipila, M.: The Role of Sulfuric Acid in Atmospheric Nucleation, Science, 2010.
Stolzenburg, D., Steiner, G., and Winkler, P. M.: A DMA-train for precision measurement of sub-10 nm aerosol dynamics, Atmospheric Measurement Techniques, 10, 1639-1651, 10.5194/amt-10-1639-2017, 2017.
Sulo, J., Sarnela, N., Kontkanen, J., Ahonen, L., Paasonen, P., Laurila, T., Jokinen, T., Kangasluoma, J., Junninen, H., Sipilä, M., Petäjä, T., Kulmala, M., and Lehtipalo, K.: Long-term measurement of sub-3 nm particles and their precursor gases in the boreal forest, Atmospheric Chemistry and Physics, 21, 695-715, 10.5194/acp-21-695-2021, 2021.
Vanhanen, J., Mikkilä, J., Lehtipalo, K., Sipilä, M., Manninen, H. E., Siivola, E., Petäjä, T., and Kulmala, M.: Particle Size Magnifier for Nano-CN Detection, Aerosol Science and Technology, 45, 533-542, 10.1080/02786826.2010.547889, 2011.
Vignati, E., Wilson, J., and Stier, P.: M7: An efficient size-resolved aerosol microphysics module for large-scale aerosol transport models, Journal of Geophysical Research: Atmospheres, 109, n/a-n/a, 10.1029/2003jd004485, 2004.
von Salzen, K., Leighton, H. G., Ariya, P. A., Barrie, L. A., Gong, S. L., Blanchet, J. P., Spacek, L., Lohmann, U., and Kleinman, L. I.: Sensitivity of sulphate aerosol size distributions and CCN concentrations over North America to SOxemissions and H2O2concentrations, Journal of Geophysical Research: Atmospheres, 105, 9741-9765, 10.1029/2000jd900027, 2000.
Wegner, T., Hussein, T., Hämeri, K., Vesala, T., Kulmala, M., and Weber, S.: Properties of aerosol signature size distributions in the urban environment as derived by cluster analysis, Atmospheric Environment, 61, 350-360, 10.1016/j.atmosenv.2012.07.048, 2012.
Whitby, K. T.: The physical characteristics of sulfur aerosols, in: Sulfur in the Atmosphere, Elsevier, 135-159, 1978.
Whitby, K. T. and Clark, W. E.: Electric aerosol particle counting and size distribution measuring system for the 0.015 to 1 μ size range 1, Tellus, 18, 573-586, 1966.
Xiao, S., Wang, M. Y., Yao, L., Kulmala, M., Zhou, B., Yang, X., Chen, J. M., Wang, D. F., Fu, Q. Y., Worsnop, D. R., and Wang, L.: Strong atmospheric new particle formation in winter in urban Shanghai, China, Atmospheric Chemistry and Physics, 15, 1769-1781, 10.5194/acp-15-1769-2015, 2015.
Yan, C., Yin, R., Lu, Y., Dada, L., Yang, D., Fu, Y., Kontkanen, J., Deng, C., Garmash, O., Ruan, J., Baalbaki, R., Schervish, M., Cai, R., Bloss, M., Chan, T., Chen, T., Chen, Q., Chen, X., Chen, Y., Chu, B., Dällenbach, K., Foreback, B., He, X., Heikkinen, L., Jokinen, T., Junninen, H., Kangasluoma, J., Kokkonen, T., Kurppa, M., Lehtipalo, K., Li, H., Li, H., Li, X.,

Liu, Y., Ma, Q., Paasonen, P., Rantala, P., Pileci, R. E., Rusanen, A., Sarnela, N., Simonen, P., Wang, S., Wang, W., Wang, Y., Xue, M., Yang, G., Yao, L., Zhou, Y., Kujansuu, J., Petäjä, T., Nie, W., Ma, Y., Ge, M., He, H., Donahue, N. M., Worsnop, D. R., Veli-Matti, K., Wang, L., Liu, Y., Zheng, J., Kulmala, M., Jiang, J., and Bianchi, F.: The Synergistic Role of Sulfuric Acid, Bases, and Oxidized Organics Governing New-Particle Formation in Beijing, Geophysical Research Letters, 48, 10.1029/2020gl091944, 2021.

Yao, L., Garmash, O., Bianchi, F., Zheng, J., Yan, C., Kontkanen, J., Junninen, H., Mazon, S. B., Ehn, M., Paasonen, P., Sipila, M., Wang, M., Wang, X., Xiao, S., Chen, H., Lu, Y., Zhang, B., Wang, D., Fu, Q., Geng, F., Li, L., Wang, H., Qiao, L., Yang, X., Chen, J., Kerminen, V. M., Petaja, T., Worsnop, D. R., Kulmala, M., and Wang, L.: Atmospheric new particle formation from sulfuric acid and amines in a Chinese megacity, Science, 361, 278-281, 10.1126/science.aao4839, 2018.

Yu, H., Hallar, A. G., You, Y., Sedlacek, A., Springston, S., Kanawade, V. P., Lee, Y. N., Wang, J., Kuang, C., and Mcgraw, R. L.: Sub-3 nm Particles Observed at the Coastal and Continental Sites in the United States, Journal of Geophysical Research: Atmospheres, 119, 860–879, 10.1002/2013JD020841, 2014.

Zhang, R., Khalizov, A., Wang, L., Hu, M., and Xu, W.: Nucleation and growth of nanoparticles in the atmosphere, Chem Rev, 112, 1957-2011, 10.1021/cr2001756, 2012.

Zhao, B., Shrivastava, M., Donahue, N. M., Gordon, H., Schervish, M., Shilling, J. E., Zaveri, R. A., Wang, J., Andreae, M. O., Zhao, C., Gaudet, B., Liu, Y., Fan, J., and Fast, J. D.: High concentration of ultrafine particles in the Amazon free troposphere produced by organic new particle formation, Proc Natl Acad Sci U S A, 117, 25344-25351, 10.1073/pnas.2006716117, 2020.

Zheng, J., Yang, D., Ma, Y., Chen, M., Cheng, J., Li, S., and Wang, M.: Development of a new corona discharge based ion source for high resolution time-of-flight chemical ionization mass spectrometer to measure gaseous H2SO4 and aerosol sulfate, Atmospheric Environment, 119, 167-173, 10.1016/j.atmosenv.2015.08.028, 2015.

Zhu, Y., Hinds, W. C., Kim, S., Shen, S., and Sioutas, C.: Study of ultrafine particles near a major highway with heavy-duty diesel traffic, Atmospheric environment, 36, 4323-4335, 2002.

525 **Table 1. The fitting parameters for the median daytime NPF, daytime non-NPF and nighttime type aerosol size distributions of four-year measurements in urban Beijing by the combination of the power law function and the lognormal distribution function.** The power law function includes two parameters, *a* and *b*. The lognormal distribution function includes the number concentration within the mode (*N*), the geometric mean diameter within the mode (d_{pg}), and the standard deviation (σ_g).

Fitting function	$\frac{\mathrm{d}N}{\mathrm{dlog}d_p} = ad_p^{-b}$		$\frac{dN}{\mathrm{dlog}d_p} = \sum_{i=1}^{n} \frac{N_i}{\sqrt{2\pi}\log\sigma_{g,i}} \exp\left[-\frac{(\log d_p - \log\bar{d}_{pg,i})^2}{2\log^2\sigma_{g,i}}\right]$								
Size range	Sub-3 nm		3-1000 nm								
Parameters	a	b	Mode 1			Mode 2			Mode 3		
			N (cm^{-3})	$\bar{d}_{pg}$ (nm)	σ_g	N (cm^{-3})	$\bar{d}_{pg}$ (nm)	σ_g	N (cm^{-3})	$\bar{d}_{pg}$ (nm)	σ_g
Daytime NPF type	1.3×10^6	6.1	1.1×10^4	3.7	1.5	1.8×10^4	9.8	1.7	6715	40.7	2.2
Daytime non-NPF type	3.8×10^4	12.2	-	-	-	9000	20.7	2.2	9900	91.7	2.0
Nighttime type	3303	16.2	-	-	-	8000	19.7	2.2	9000	85.0	2.0

530

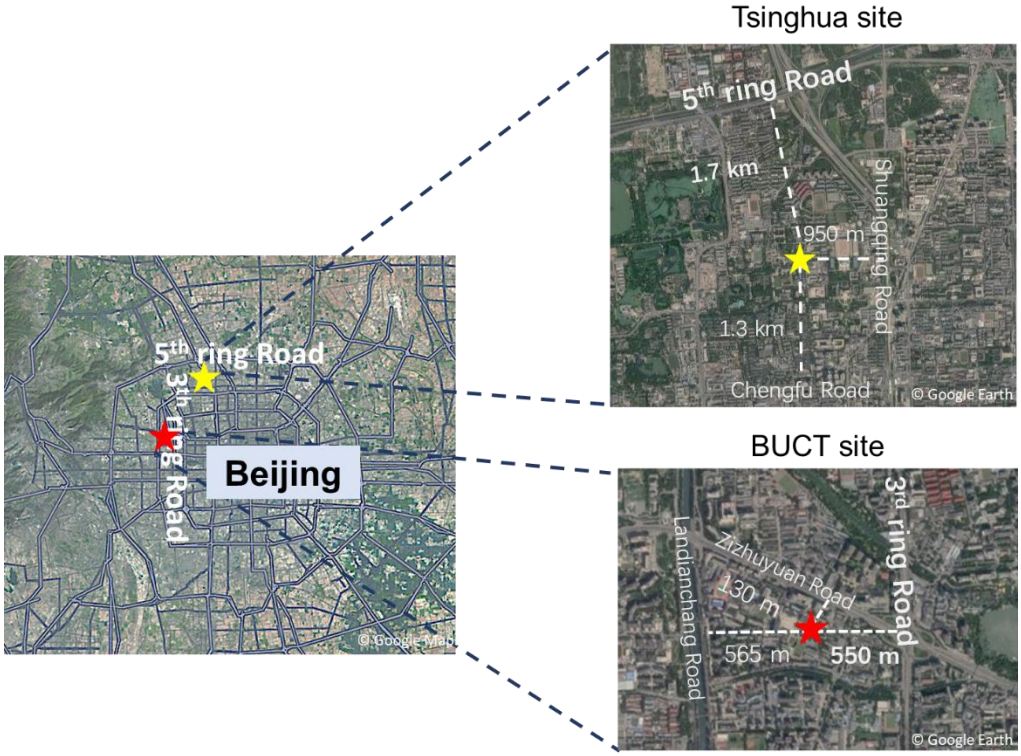

Figure 1. The locations of two measurement sites in urban Beijing, i.e., Tsinghua site (yellow star) and BUCT site (red star). The BUCT site is more influenced by the traffic emissions. The main roads and their distance from the measurement sites are marked in the figure. 5th ring road and 3rd ring road are the main roads near the Tsinghua site and the BUCT site, respectively. The maps are from Google Maps and Google Earth.

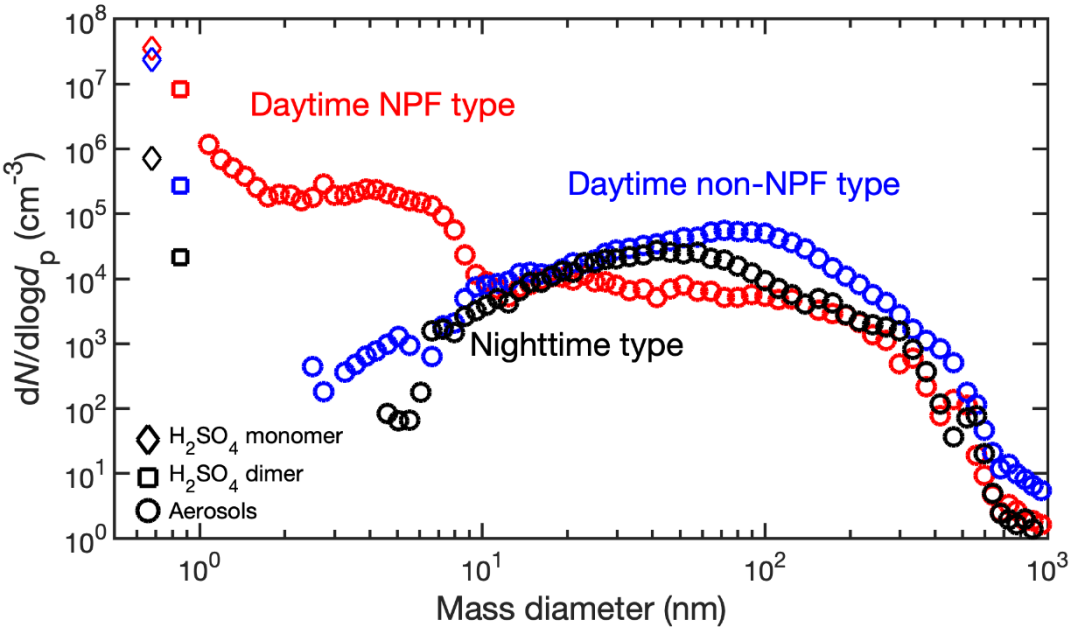

Figure 2. Cases of three typical types of number size distributions from H_2SO_4 monomer to dimer and then to larger aerosol size: the daytime NPF type (red), daytime non-NPF type (blue) and nighttime type (black). The daytime NPF, daytime non-NPF and nighttime PNSD is selected during the NPF period on a NPF day (Feb. 16 11:10, 2018), during the daytime on a non-NPF day (Feb. 25 12:25, 2018) and during the nighttime (Apr. 4 00:35, 2018). The diamonds, squares, and circles represent the distribution function ($dN/d\log d_p$) of H_2SO_4 monomers, dimers, and aerosols, respectively.

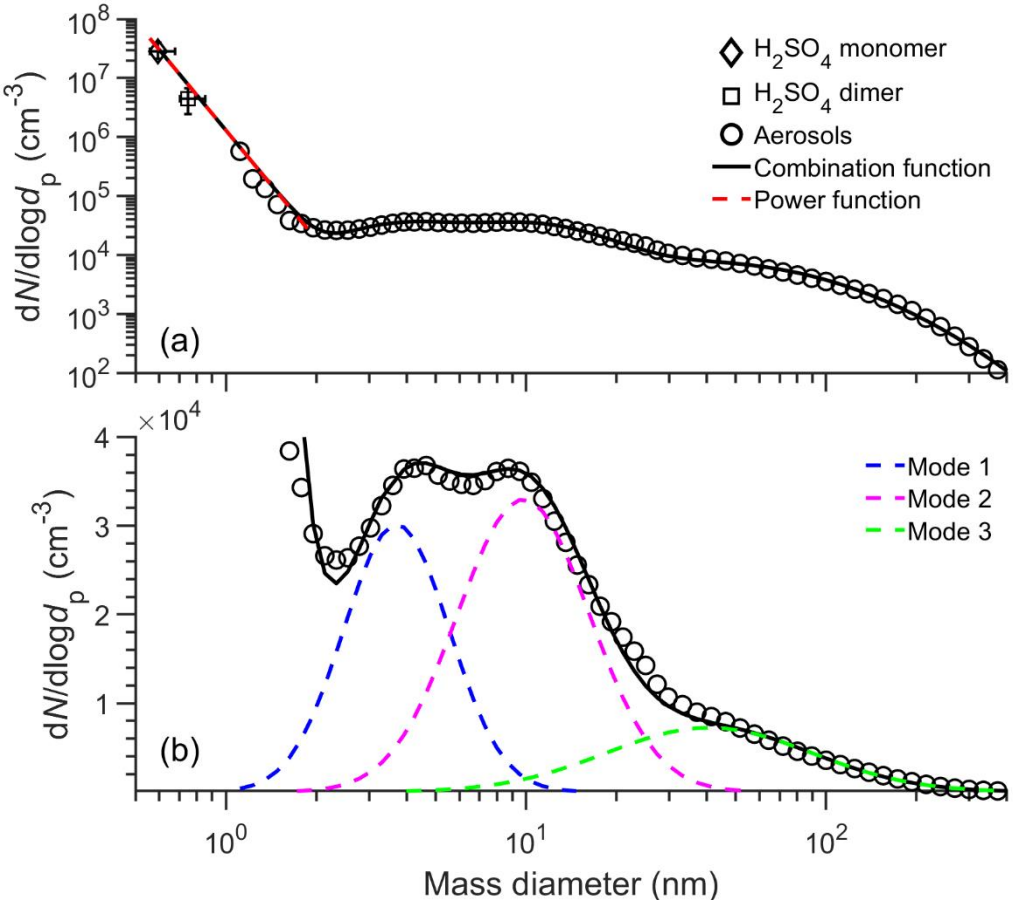

Figure 3. The median daytime NPF type number size distributions from H_2SO_4 monomer to larger aerosols and the fitted size distributions shown in (a) logarithm scale and (b) linear scale of y axis. The x-axis error bars of H_2SO_4 monomers and dimers indicate the variation range of estimated H_2SO_4 monomers and dimers diameters by assuming the bulk density to be 1000~1800 kg m^3. The y-axis error bars of H_2SO_4 monomers and dimers indicate the 25^{th}~75^{th} range of concentrations. The black and red lines indicate the fitted size distribution in the whole size range and in sub-3 nm size range, respectively. The blue, magenta and green lines present the fitted mode 1, mode 2 and mode 3, respectively. The diamonds, squares, and circles represent the distribution function ($dN/d\log d_p$) of H_2SO_4 monomers, dimers and aerosols, respectively.

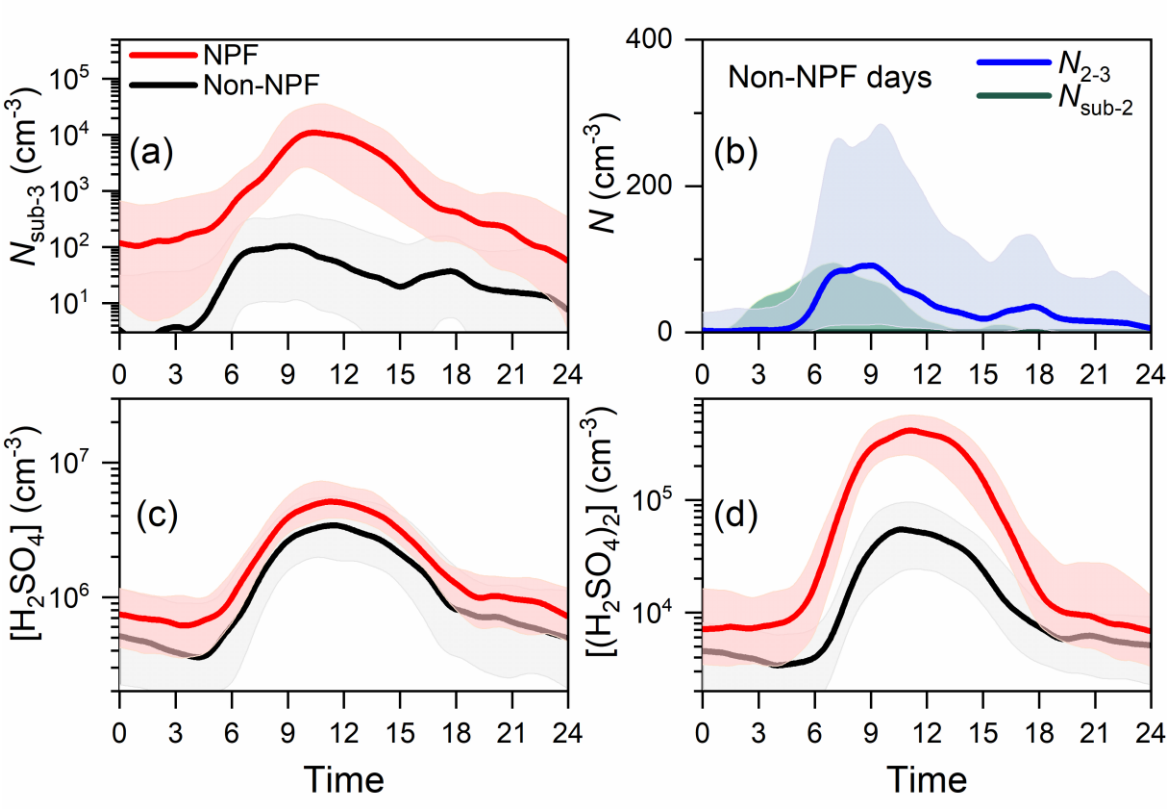

Figure 4. The diurnal variations of (a) number concentration of sub-3 nm aerosols (N_{sub-3}), (c) H_2SO_4 monomer concentration and (d) H_2SO_4 dimer concentration on NPF days and non-NPF days. (b) The diurnal variations of number concentration of sub-2 nm aerosols (N_{sub-2}) and 2-3 nm aerosols (N_{2-3}) on non-NPF days. The solid lines represent median values and the shading areas indicate 25th – 75th percentiles. Note that the median diurnal variations of N_{sub-2} are near zero on non-NPF days in (b).

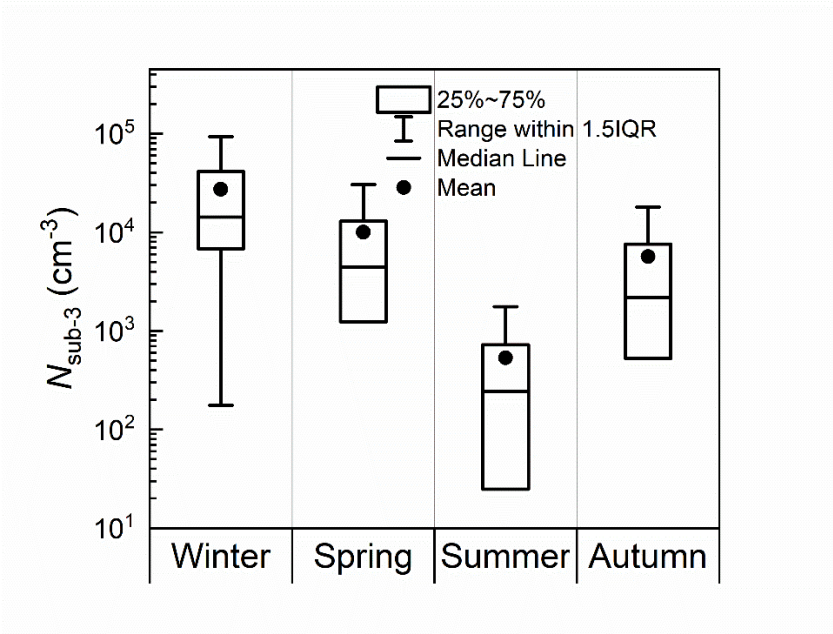

Figure 5. The seasonal variations of number concentrations of sub-3 nm aerosols (N_{sub-3}) on NPF days in urban Beijing. Data during 9:00 – 14:00 were shown in this figure. The vertical lines and circles in the box indicate the median and mean values, respectively. The top and bottom edges represent 75th and 25th percentiles, respectively. The IQR is the interquartile range.

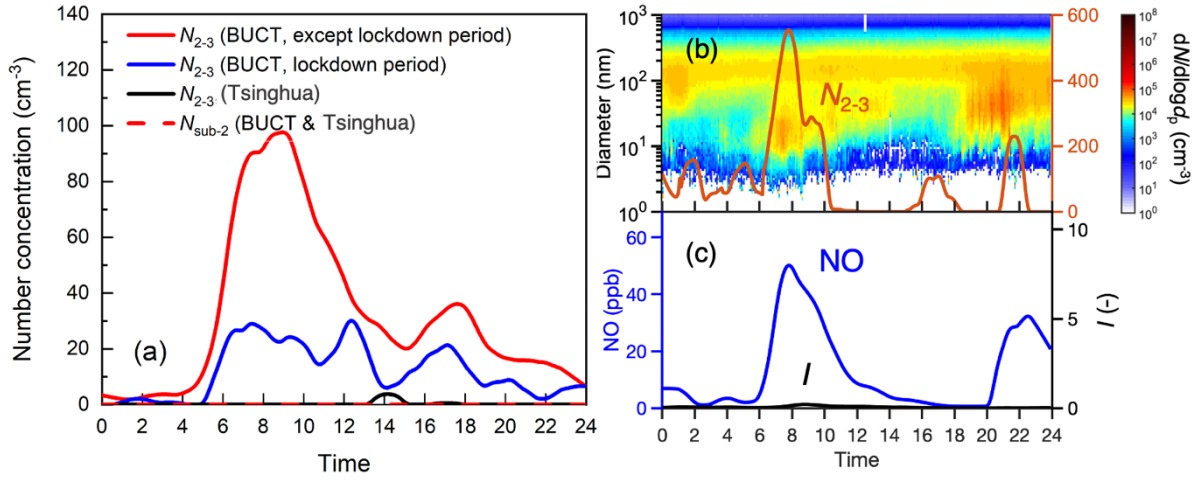

575 **Figure 6. (a) Median diurnal variations of number concentrations of 2-3 nm aerosols (N_{2-3}) on non-NPF days at the BUCT site during COVID-19 lockdown period (Jan. 24, 2020 – Feb. 25, 2020) and other time period (except lockdown period), and at the Tsinghua site (Mar. 7, 2016 – Apr. 6, 2016).** The median diurnal variations of number concentrations of sub-2 nm aerosols (N_{sub-2}) are near zero on non-NPF days at both BUCT and Tsinghua sites. The temporal pattern of (b) aerosol size distributions, N_{2-3}, (c) NO concentration and the indicator I on a non-NPF day (Mar. 13, 2018).

580